

# Close Encounter of Three Black Holes III

Giuseppe Ficarra and Carlos O. Lousto

*Center for Computational Relativity and Gravitation,  
School of Mathematical Sciences, Rochester Institute of Technology,  
85 Lomb Memorial Drive, Rochester, New York 14623, USA*

(Dated: June 19, 2024)

We revisit the three black hole scenario with numerical relativity techniques to study hierarchical configurations where the inner binary contains highly spinning black holes. We find that the merger time of the binary gets a delay (with a number of orbits to merger increase), depending strongly with the distance to the orbiting third hole  $D$  as  $\sim 1/D^{1.6\pm 0.1}$ . Notably, a different dependence from what we had found in the nonspinning case,  $\sim 1/D^{2.5}$ . We interpret this effect as mostly due to a spin-orbit coupling between the third hole and the closest member of the binary in the successive approaches. This lead us next to study scattering configurations of the third hole with the binary in order to evaluate the extent of this “sudden” interactions, finding also a correlation of the delay in merger times with the closest distance, even for the nonspinning cases. We then explore the mass ratio dependence of the triple system by modeling binaries orbiting a larger black hole bearing masses ratios 8:1:1 and 18:1:1 in co-orbiting or counter-orbiting configurations, finding merger times increasing with increasing mass ratios and for the counter-orbiting cases.

PACS numbers: 04.25.dg, 04.25.Nx, 04.30.Db, 04.70.Bw

## I. INTRODUCTION

There is a renewed interest in the study of multi black hole interactions, in particular the effect a third black hole may have on a close binary. Three body encounters and accretion effects (see, e.g., [1–5]) can lead to highly eccentric binaries, with residual eccentricity surviving down to near merger. These eccentric binaries may have very interesting gravitational waves signals that cannot be adequately modeled using quasicircular approximations [6]. This subject has been the focus of much interest lately [7–9], but its detailed modeling is largely incomplete. Reliable evolutions that include those effects between LISA and third generation detectors sensitivity bands can also be used to exploit multiband observational opportunities [10–14].

This paper is the third installment of the three black hole interactions study using full Numerical General Relativity techniques. In a first paper [15] we have performed a set of proofs of principle evolutions to show that effectively our moving punctures approach [16] can evolve accurately multi black hole systems beyond binaries. Next we have revisited the three black hole (3BH) scenario in [17] to study the influence of a third hole on eccentricity generation during evolution and merger times of an inner nonspinning binary. While the eccentricity evolution seemed mostly unaffected, presenting a steady decay, the merger times could be modeled with a distance  $D$ , to the third hole as a dependence  $\approx 1/D^{2.5}$ .

In this paper we complete our intended trilogy of 3BH studies, by revisiting the scenario of the third hole interacting with an inner binary, this time with highly spinning black holes to see if the previous results regarding merger time and eccentricity evolutions still stands. We will also consider here the effects of a scattering third

hole instead of in bound orbits and finally the effects of a much more massive central third hole with a binary orbiting around it.

## II. FULL NUMERICAL TECHNIQUES

In order to perform the full numerical simulations of three black holes we employ the LazEv code [18] including 8th order spatial finite differences [15], 4th order Runge-Kutta time integration, and a Courant factor ( $dt/dx = 1/4$ ).

Regularly to compute the numerical initial data for binary black holes, we use the puncture approach [19] along with the TWO PUNCTURES [20] code, that we will use in a hybrid approach in this paper as described in next Sec. III. We use the AHFINDERDIRECT [21] code to locate apparent horizons and compute horizon masses from its area  $A_H$ . We also measure the magnitude of the horizon spin  $S_H$ , using the “isolated horizon” algorithm as implemented in Ref. [22].

During evolution of the holes we use the CARPET [23] mesh refinement driver which provides a “moving boxes” style of mesh refinement. In this approach, refined grids of fixed size are arranged about the coordinate centers of the holes. The code then moves these fine grids about the computational domain by following the trajectories of the black holes.

The grid structure of our mesh refinements have a size of the largest box for typical simulations of  $\pm 400M$ . The number of points between 0 and 400 on the coarsest grid is XXX in nXXX (i.e. n100 has 100 points). So, the grid spacing on the coarsest level is  $400/XXX$ . The resolution in the wavezone is  $100M/XXX$  (i.e. n100 has  $M/1.00$ , n120 has  $M/1.2$  and n144 has  $M/1.44$ ) and the rest of

the levels is adjusted globally. For comparable masses and non-spinning black holes, the grid around one of the black holes ( $m_1$ ) is fixed at  $\pm 0.8M$  in size and is the 9th refinement level. Therefore the grid spacing at this highest refinement level is  $400/\text{XXX}/2^8$ . When considering small mass ratio binaries, we progressively add internal grid refinement levels [24]. In the case of spinning black holes we add an additional refinement level inside the black hole apparent horizon and we increase the global resolution to n120.

The extraction of gravitational radiation from the numerical relativity simulations is performed using the formulas (22) and (23) from [25] for the energy and linear momentum radiated, respectively, and the formulas in [26] for angular momentum radiated, all in terms of the extracted Weyl scalar  $\Psi_4$  at the observer location  $R_{obs} = 113M$ .

### III. APPROXIMATE INITIAL DATA

In Ref. [17] we have performed three black holes evolution studies from full approximate initial data based on work in [15], which extended first order expansion to include terms of the sort  $\vec{S}_i \times \vec{P}_i$  representing interactions of spin with linear momentum, to higher order on those intrinsic parameters of the holes,  $\vec{S}_i$  and  $\vec{P}_i$  as well as the inverse of the distance of the holes.

Since in the Bowen-York approach to initial data [27], with the ansatz of conformal flatness of the three-metric and transverse traceless of the extrinsic curvature, the momentum constraint is solved exactly, we have to look for a perturbative solution of the Hamiltonian constraint equation, reduced to the partial differential equation for the conformal factor  $\phi$

$$\Delta\phi = -\frac{1}{8}\phi^{-7}\hat{A}^{ij}\hat{A}_{ij}, \quad (1)$$

with the Bowen-York conformal extrinsic curvature solution to the momentum constraint

$$\hat{A}^{ij} = \sum_a^{N_{BHs}} \left( \frac{3}{2r_a^2} \left[ 2P_a^{(i}n_a^{j)} + (n_a^i n_a^j - \eta^{ij})P_{ak}n_a^k \right] + \frac{6}{r_a^3} n_a^{(i}\epsilon^{j)kl} J_{ak}n_{al} \right), \quad (2)$$

where we label the momentum and the spin of the holes as  $\mathbf{P}_i$  and  $\mathbf{J}_i$ , following the notation of [15].

For the purpose to find an approximate solution to the Hamiltonian constraint we start from the analytical solution at order 0th given by

$$\phi_0 = 1 + \sum_a^{N_{BHs}} \frac{m_a}{2r_a}, \quad (3)$$

which solves

$$\Delta\phi_0 = 0. \quad (4)$$

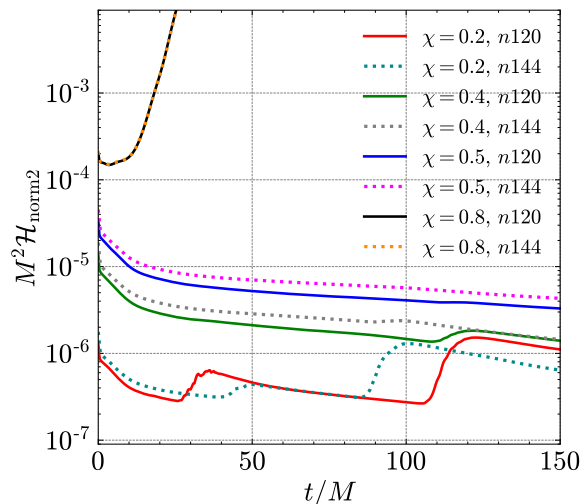


FIG. 1. Evolution of the L2-norm of the Hamiltonian constraint for the two black holes approximate initial data for spinning holes at increasing global finite differences resolution.

To find the first perturbative order  $u$  of the solution defined as

$$\phi = \phi_0 + u, \quad (5)$$

we consider the equation for  $u_1$

$$\Delta u_1 = -\frac{1}{8}\phi_0^{-7}\hat{A}^{ij}\hat{A}_{ij}. \quad (6)$$

Then to solve for the second order piece  $u_2$ , we look at the perturbation equation for a single black hole we have [17],

$$\Delta u_2 = \frac{7}{8}\phi_0^{-8}u_1\hat{A}^{ij}\hat{A}_{ij}. \quad (7)$$

In Ref. [17] we have superposed those perturbative solutions to the Hamiltonian constraint to study the evolution of three equal mass, nonspinning, black hole systems in a hierarchical configuration consisting of a close binary with a third hole in coplanar as well as in polar and other precessing cases. Here we would like to revisit the problem in the case the black holes in the inner binary carry a significant spin.

A study of our perturbative initial data, applied to an equal mass and equal aligned spins binary systems with increasing intrinsic spins magnitude,  $\chi = S_i/m_i^2$ , is displayed in Fig 1, showing the control on the violations of the Hamiltonian constraint during evolution for up to medium magnitudes of the spins. We also observe the increase of the levels of violation of the Hamiltonian constraint with the magnitude of the spins and the lack of reduction of the violations with increasing global numerical resolution, leading to the conclusion that those violations are due to the errors produced by the approximation expansion itself.

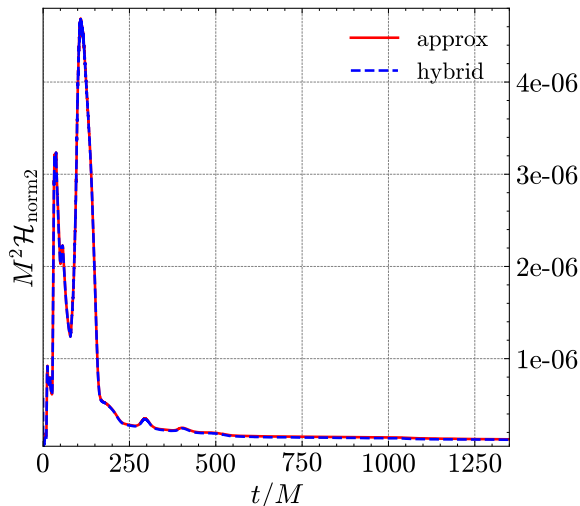


FIG. 2. Comparative evolution of the violations of the Hamiltonian constraint for three nonspinning black holes in the full approximation for initial data and for the hybrid exact solution for two black holes and the third approximated.

Specifically, when we try to increase the value of the spins above a perturbative regime  $\chi > 0.5$ , we see the restrictions of this approach applied to highly spinning holes as displayed in the black and orange lines of Fig. 1 for the case of  $\chi = 0.8$ . This naturally indicates the limitations of the perturbative expansion to represent large values of the spin magnitude.

This suggested us to adopt a hybrid approach to the initial data problem by solving the highly spinning binary with the usual full numerical approach, i.e. the TWOPUNCTURES [20] code and then superpose to that solution the third hole in an approximate way. We test such approach by reproducing the 3BH1 setup of [17], finding consistent results during evolution as displayed in Fig. 2 for the Hamiltonian constraint and for the tracks of the three black hole orbits as shown in Fig. 3.

We thus conclude that we can use the hybrid approach to the initial data problem to study evolutions of spinning inner binaries with a third nonspinning hole in the hierarchical configurations of interest. We note that full numerical solutions to three black holes initial data have been studied in Refs. [28–30] but we found our method more practical to implement for exploratory studies.

#### IV. THREE BLACK HOLES EVOLUTIONS

In this new exploration we will consider a hierarchical prototypical system with the inner binary at an initial separation of  $12m = 8M$  and a third black hole at separation  $30M$  (where  $m = m_1^H + m_2^H$ , the addition of the horizon masses of the binary, and  $M = m_3^H + m$ , the addition of all three horizon masses). All black holes in this first set will have equal masses (as measured by their

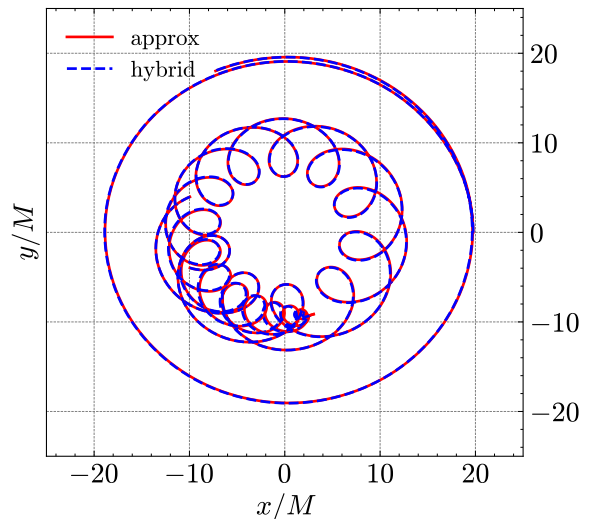


FIG. 3. Comparative evolution of the orbital trajectories for three nonspinning black holes in the full approximated initial data and the hybrid exact solution for two black holes plus the third approximated.

individual horizons) and different relative orbital orientations. Additionally, the inner binary will have individual spin components  $\chi_1 = \chi_2 = +0.8$  along the  $z$ -axis. This set up is depicted in Fig. 4. In order to work with small initial eccentricities we consider the inner binary as isolated and use the quasicircular formulas of Ref. [31] to obtain the parameters reported in the first column of Table I and referred to as 2BH0s. After getting the inner binary parameters we apply the same quasicircular criteria to the outer orbit of the third black hole with a single effective spinning hole having the added masses and total angular momentum of the inner binary. This process provides low enough eccentricities ( $e \lesssim 0.05$ ) for the purposes of our initial study.

##### A. Hierarchical Three black holes configurations

To start exploring this vast parameter space we have chosen to consider two coplanar cases, when the third black hole orbit is co-orbiting with the binary (3BH1s) and when it is counter-orbiting (3BH2s). Those parameters are given in Table I. We also consider a precessing case with the third black hole momentum perpendicular to the orbital plane of the binary (3BH3s), as depicted in Fig. 4. In all cases we considered the quasicircular orbit of the third black hole with the inner binary as an effective single black hole as described above.

In Fig. 5 we display the extracted waveform of the three black hole simulation 3BH1s. The gravitational radiation is completely dominated by the inner binary. The difference with an isolated binary is given by the delay in the merger due to the presence of the third black hole. Similar results are obtained for the 3BH2s case, as seen in the

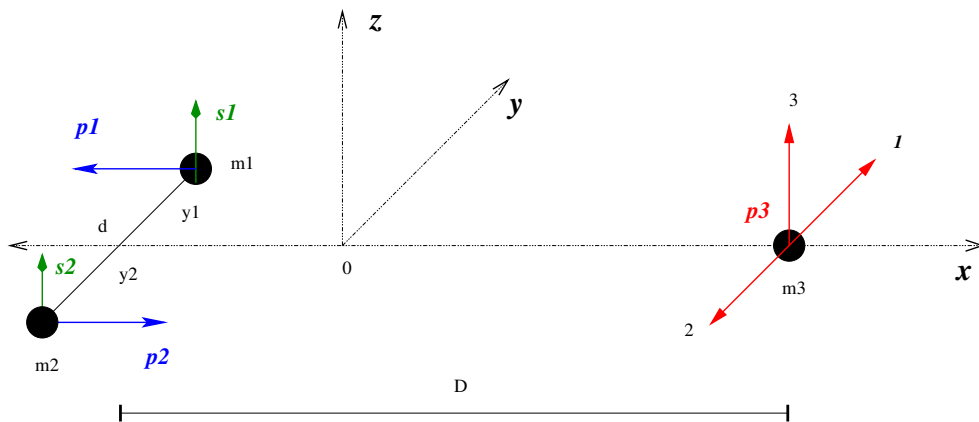


FIG. 4. Initial configurations considered for the three black hole evolutions, labeled as 3BH1s, 3BH2s, for coplanar co- and counter- orbiting, and 3BH3s for polar.

bottom of Fig. 5. The eccentricity of the 3BH cases is already apparent in the waveform amplitude versus time in comparison with the 2BH isolated binary. This eccentricity effect will also reflect in the tracks of the holes as we will display below. Another effect is the orbital motion of the binary and its merger remnant around the center of mass of the triple system, as displayed in Figs. 6 and 7, due to the asymmetric gravitational radiation of an unequal mass systems. This displacement leads to a mixing of the gravitational waves modes as seen at a fixed observer location, but its effects can be disentangled with techniques like those used in Refs. [32, 33]. The polar case 3BH3s gives a qualitative and quantitative close picture to these cases, serving as a sort of control of the differences expected due to precession. Fig. 9 displays the comparative evolution of the inner binary separation in all these three cases. We note here that a polar and other two precessing cases have been studied in our previous paper Ref. [17] for the nonspinning binaries and again did not display qualitatively new features, with results being bracketed between the polar and coplanar cases.

The relative motion of the inner binary can be tracked during evolution of the three black hole system. We can observe comparable initial trajectories and eccentricities (much larger than in the isolated binary case 2BH0s), and similar larger merger times for 3BH3s and 3BH1s while the counter-orbiting 3BH2s delays merger by about  $\sim 100M$ .

We can evaluate eccentricity during evolution via the simple formula, as a function of the separation of the holes,  $d$ ,  $e_d = d^2 \dot{d}/m$ , as given in [34]. We can thus monitor the eccentricity evolution of the orbit of the third black hole. Before the binary's merger we can refer the distance of the third hole to the center of mass of the binary system, as displayed in the bottom of Fig. 6 and 7, and then after the merger of the the inner binary to its remnant, as displayed on the right panel of Fig. 8. We note that the eccentricity measure from the center of mass of the binary has some total amplitude oscillations

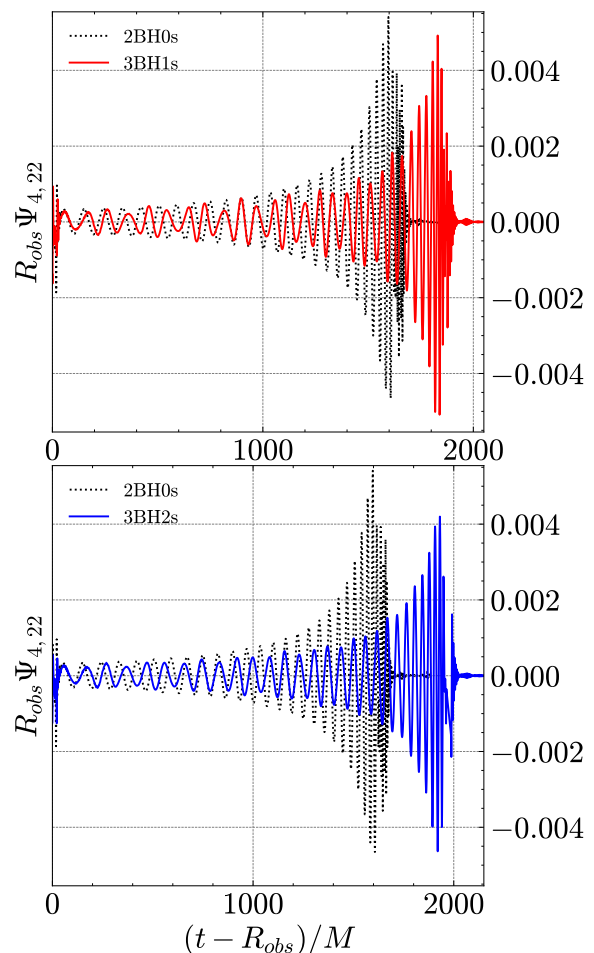


FIG. 5. Waveforms generated by the co- and counter- orbiting cases 3BH1s and 3BH2s in comparison with the isolated binary 2BH0s. Note the effects of eccentricity in the amplitude and post binary merger. Here  $R_{obs} = 113M$  and (2,2) modes extracted.

TABLE I. Initial data parameters for the base binary (2BH0s), two coplanar (3BH1s, 3BH2s) and polar (3BH3s) configurations with a third black hole at a distance  $D$  from the binary along the  $x$ -axis.  $(x_i, y_i, z_i)$  and  $(p_i^x, p_i^y, p_i^z)$  are the initial position and momentum of the puncture  $i$ ,  $m_i^p$  is the puncture mass parameter,  $m_i^H$  and  $\chi_{iz}^H$  are the horizon mass and dimensionless spin at  $t = 0$ ,  $M\Omega$  is the binary's orbital frequency,  $d$  is the binary's initial coordinate separation and  $d_{spd}$  is the binary's proper distance. Parameters not specified are zero.

Config	2BH0s	3BH1s	3BH2s	3BH3s
$x_1/M$	-9.94446878	-9.94446878	-9.99075115	-9.96704932
$y_1/M$	3.96250893	3.96250893	3.96250893	3.96250893
$z_1/M$	0.00000000	0.00000000	0.00000000	0.00000000
$p_1^x/M$	-0.05463934	-0.05462799	-0.05462652	-0.05462799
$p_1^y/M$	-0.03157750	-0.02172902	0.02175594	-0.00031577
$p_1^z/M$	0.00000000	0.00000000	0.00000000	-0.02169541
$m_1^p/M$	0.20246647	0.20012400	0.20010400	0.20010600
$m_1^H/M$	0.33147290	0.33152795	0.33152152	0.33152582
$\chi_{1z}^H/M$	0.80906581	0.80880423	0.80883273	0.80880178
$x_2/M$	-9.94446878	-9.94446878	-9.99075115	-9.96704932
$y_2/M$	-3.96250893	-3.96250893	-3.96250893	-3.96250893
$z_2/M$	0.00000000	0.00000000	0.00000000	0.00000000
$p_2^x/M$	0.05463934	0.05465069	0.05465216	0.05708188
$p_2^y/M$	0.03157750	-0.02109747	0.02238748	0.00036813
$p_2^z/M$	0.00000000	0.00000000	0.00000000	-0.02166824
$m_2^p/M$	0.20246647	0.20012400	0.20010400	0.20010600
$m_2^H/M$	0.33147321	0.33152655	0.33152212	0.33152648
$\chi_{2z}^H/M$	0.80906785	0.80881193	0.80881481	0.80880501
$d/M$	7.92501785	7.92501785	7.92501785	7.92501785
$d_{spd}/M$	11.0475159	11.1643519	11.1545122	11.1645980
$x_3/M$		19.9492516	19.9054250	19.9277120
$y_3/M$		0.00000000	0.00000000	0.00000000
$z_3/M$		0.00000000	0.00000000	0.00000000
$p_3^x/M$		-0.00002269	-0.00002564	-0.00002269
$p_3^y/M$		0.04282649	-0.04414343	0.00000000
$p_3^z/M$		0.00000000	0.00000000	0.04339083
$m_3^p/M$		0.32906500	0.32902500	0.32902500
$m_3^H/M$		0.33332869	0.33333254	0.33330730
$M\Omega$	0.032314209	0.00581907	0.00587723	0.00583637
$D/M$		29.8937203	29.8961761	29.8947610

with the third black hole orbit and also seems to grow in time reaching relatively large values before merger. This seems to be an effect of the use of the coordinates of the center of mass as a reference for this extended system. We note that right after merger the eccentricity measure produces an order of magnitude smaller eccentricity for the subsequent two orbits of the simulation and produce values more in line with what we expect and found for the inner binary studies above.

### B. Distance dependence to the third black hole

We next explore how the merger times and eccentricity evolution of the inner binary vary versus the initial separation of the outer black hole in our hierarchical setups. For that end we look again for quasi-circular effective parameters at different initial separa-

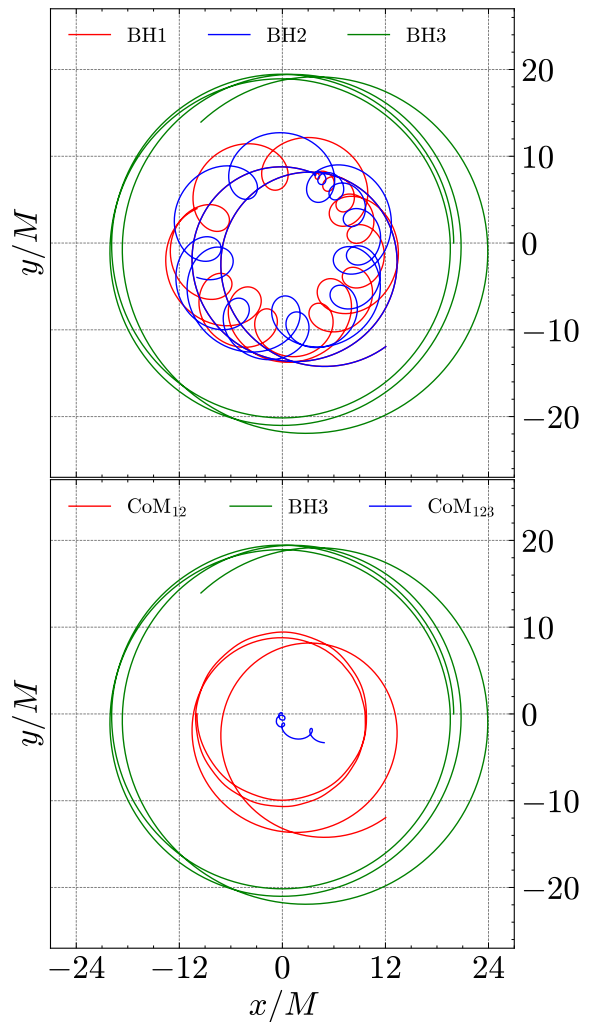


FIG. 6. Trajectories of the coplanar co-orbiting case 3BH1s and the evolution of the center of masses of the binary and of the three black holes. Note the kick after merger.

tions beyond the reference one at  $D = 30M$  (reabeled as 3BH1sD0 and 3BH2sD0) at increasing initial separations  $D/M = 35, 40, 50, 60$ , that we label 3BH1sD1-4 and 3BH1sD1-4 as given in Tables II and III

We are interested in studying the effect the third hole has on the inner binary dynamics. In particular on how it affects the merger, if prompts or delays it. In Table IV we give the results of our simulations versus the initial third black hole distance to the binary's center of mass. We find a clear trend towards the delay of the merger, in both quantities, the merger time and the number of orbits as measured by the tracks of the holes, where we used as a definition of merger when the binary distance reaches  $d = 0.7M$  (which corresponds closely to the formation of a common horizon).

We model the merger delay as a function of the initial distance to the third black hole and consider deviations with respect to the merger time and number of orbits to merger of the isolated binary, 2BH0s. We

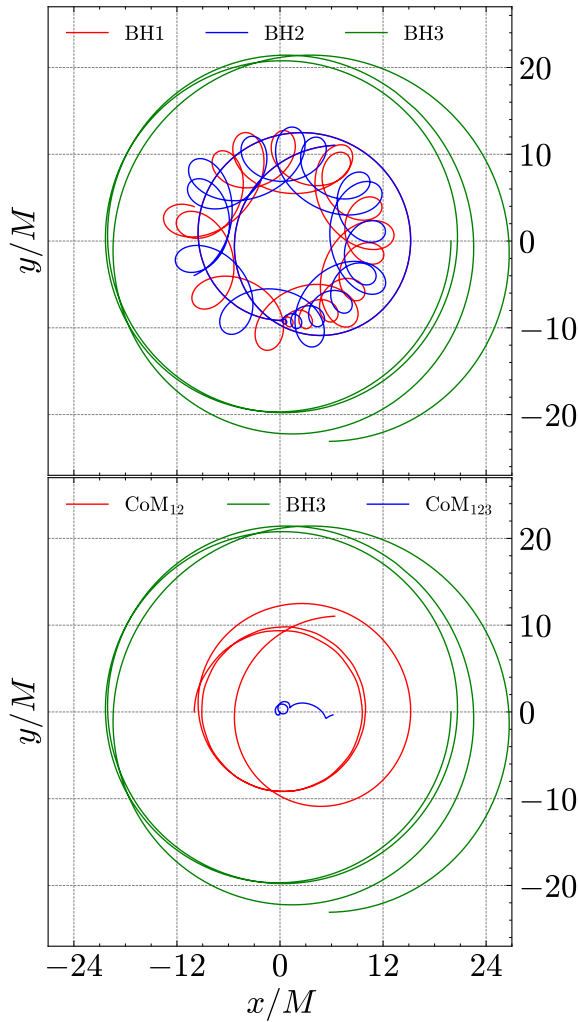


FIG. 7. Trajectories of the coplanar counter-orbiting case 3BH2s and the evolution of the center of masses of the binary and of the three black holes. Note the effects of the kick after merger.

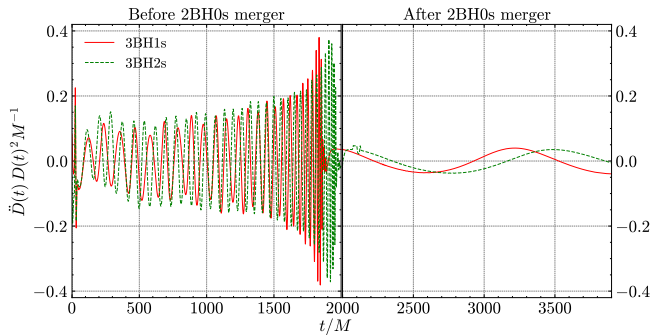


FIG. 8. Eccentricity evolution of the outer black hole as measured by  $D^2 \dot{D}(t)/M$  for the triple black hole coplanar cases 3BH1s-2s and its transition after the inner binary (2BH0s) merger.

TABLE II. Initial data parameters for coplanar configurations with a third black hole placed at different distances  $D$  from the binary along the  $x$ -axis, 3BH1sD1-4.

Config	3BH1sD1	3BH1sD2	3BH1sD3	3BH1sD4
$x_1/M$	-11.612696	-13.280575	-16.6156958	-19.9503036
$y_1/M$	3.96250893	3.96250893	3.96250893	3.96250893
$p_1^x/M$	-0.05463218	-0.05463453	-0.05463687	-0.05463791
$p_1^y/M$	-0.02000458	-0.01863566	-0.01657699	-0.01508252
$m_1^p/M$	0.20052900	0.20080000	0.20128000	0.20145000
$m_1^H/M$	0.33154561	0.33154757	0.33158544	0.33155661
$\chi_{1z}^H/M$	0.80869972	0.80868571	0.80850782	0.80863483
$x_2/M$	-11.612696	-13.280575	-16.6156958	-19.9503036
$y_2/M$	-3.96250893	-3.96250893	-3.96250893	-3.96250893
$p_2^x/M$	0.05464651	0.05464415	0.05464181	0.05464078
$p_2^y/M$	-0.01937303	-0.01800411	-0.01594544	-0.01445097
$m_2^p/M$	0.20052900	0.20080000	0.20128000	0.20145000
$m_2^H/M$	0.33154384	0.33154772	0.33158381	0.33155726
$\chi_{2z}^H/M$	0.80870507	0.80870384	0.80851186	0.80865377
$d/M$	7.92501785	7.92501785	7.92501785	7.92501785
$d_{spd}/M$	11.1475754	11.1350617	11.1172208	11.1056409
$x_3/M$	23.2803971	26.6120360	33.27622481	39.94114485
$y_3/M$	0.00000000	0.00000000	0.00000000	0.00000000
$p_3^x/M$	-0.00001433	-0.00000962	-0.00000495	-0.00000287
$p_3^y/M$	0.03937762	0.03663976	0.03252242	0.02953350
$m_3^p/M$	0.32965000	0.33009500	0.33120500	0.33120500
$m_3^H/M$	0.33331060	0.33330102	0.33331759	0.33334524
$M\Omega$	0.00464832	0.00382336	0.002754558	0.002104978
$D/M$	34.8930391	39.8926110	49.8919206	59.89144850

TABLE III. Initial data parameters for coplanar configurations with a third black hole placed at different distances  $D$  from the binary along the  $x$ -axis, 3BH2sD1-4.

Config	3BH2sD1	3BH2sD2	3BH2sD3	3BH2sD4
$x_1/M$	-11.6543899	-13.3187754	-16.6488714	-19.9799919
$y_1/M$	3.96250893	3.96250893	3.96250893	3.96250893
$p_1^x/M$	-0.05463145	-0.05463414	-0.05463673	-0.05463784
$p_1^y/M$	0.01985426	0.01837108	0.01617898	0.01461254
$m_1^p/M$	0.20053000	0.20080000	0.20128000	0.20145000
$m_1^H/M$	0.33154688	0.33154740	0.33158433	0.33155782
$\chi_{1z}^H/M$	0.80870397	0.80868774	0.80850861	0.80865279
$x_2/M$	-11.6543899	-13.3187754	-16.6488714	-19.9799919
$y_2/M$	-3.96250893	-3.96250893	-3.96250893	-3.96250893
$p_2^x/M$	0.05464723	0.05464454	0.05464195	0.05464084
$p_2^y/M$	0.02048581	0.01900263	0.01681053	0.01524409
$m_2^p/M$	0.20053000	0.20080000	0.20128000	0.20145000
$m_2^H/M$	0.33154769	0.33154828	0.33158463	0.33156030
$\chi_{2z}^H/M$	0.80868914	0.80867610	0.80849371	0.80865465
$d/M$	7.92501785	7.92501785	7.92501785	7.92501785
$d_{spd}/M$	11.14783586	11.12480118	11.10687866	11.105719020
$x_3/M$	23.2406336	26.5754054	33.2441618	39.9122978
$y_3/M$	0.00000000	0.00000000	0.00000000	0.00000000
$p_3^x/M$	-0.00001577	-0.00001040	-0.00000523	-0.00000299
$p_3^y/M$	-0.04034007	-0.03737370	-0.03298950	-0.02985663
$m_3^p/M$	0.32965000	0.33009500	0.33075000	0.33120500
$m_3^H/M$	0.33334044	0.33332222	0.33332950	0.33335266
$M\Omega$	0.00468542	0.003848442	0.002767571	0.002112571
$D/M$	34.8950235	39.8941808	49.8930332	59.8922897

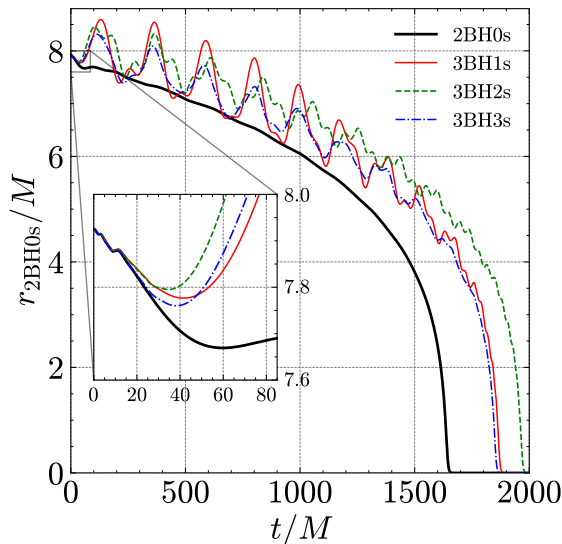


FIG. 9. Relative separation of the inner binary versus time of the three black hole cases studied here 3BH1s-3s in comparison with the isolated binary case. Delayed merger and higher eccentricity effects are evident.

then fit a dependence to the data in Table IV of the form  $2\text{BH}0s + a_1/D^{a_2}$  for the four larger separation cases 3BH1,2sD1-4. The results are displayed in Fig. 10 for the third hole co- and counter- orbiting with respect to the inner binary orbital momentum respectively. We found in both cases, that a fit leads to a consistent dependence of the form  $\sim 1/D^{1.6 \pm 0.1}$ . This is verified when seen in terms of the number of orbits as well as the evolution time at the top and bottom of both curves. Note also the consistent approach of the curves towards a common value (the isolated binary's) at large separation of the third hole for both configurations. Had we included the  $D = 30$  cases in the fits, we would still find a  $-1.6$  power dependence, but with larger deviations,  $\sim 1/D^{1.6 \pm 0.2}$ .

In Table IV we report the merger times and number of orbits for the five cases studied here and the two orbital orientations 1s and 2s. We first note the clear delay of the merger of 3BHD0-4 with respect to the isolated binary 2BH0s. We next note the near  $1/D^{1.6}$  dependence of the merger times and number of orbits with initial separation of the third hole,  $D$ , and the convergence to the isolated binary results for large initial separations of the third hole. We finally note the systematic further merger delay for the counter-orbiting configuration with respect to the co-orbiting one.

## V. OTHER THREE BLACK HOLE CONFIGURATIONS

In this section we explore two other 3BH configurations of potential astrophysical interest, the case of a third black hole in a close scattering trajectory with respect to

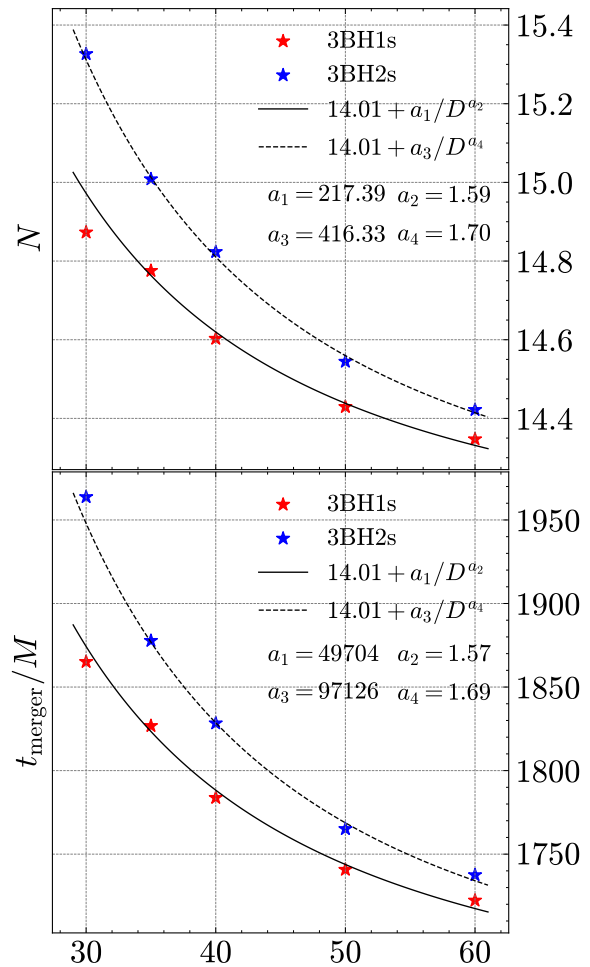


FIG. 10. Fit to a functional dependence  $2\text{BH}0s + a_{1,3}/D^{a_{2,4}}$  for the coplanar, co-orbiting 3BHs1D1-4 and counter-orbiting 3BHs2D1-4 configurations versus distance  $D/M$  of the third hole. The  $D = 30M$  points are displayed but not fitted.

TABLE IV. Number of orbits to merger and merger time of the inner binary for different orbital distances of the third black hole. Cases 3BHD0-4 where (1s) is prograde and (2s) retrograde orbits.

$D/M$	#orbits (1s)	$t_{\text{merger}}/M$ (1s)	#orbits (2s)	$t_{\text{merger}}/M$ (2s)
30	14.87	1865.10	15.33	1963.75
35	14.78	1826.77	15.00	1877.71
40	14.60	1783.75	14.82	1828.33
50	14.43	1740.73	14.54	1765.10
60	14.35	1722.29	14.42	1737.50
$\infty$	14.01	1638.02	14.01	1638.02

a binary, and the case of a binary orbiting a more massive third black hole.

### A. Scattering Three black holes configurations

We have seen that our studies of three black hole evolutions indicate some evidence that those three body interactions seem to be dominated by the closest or 'sudden' approach of one component of the inner binary to the third hole. In order to further explore this hypothesis we can try to single out this 'sudden' effect by studying configurations where the third black hole approaches the binary in a close scattering orbit.

In order to simplify the analysis and to relate the scattering orbits to the previous quasicircular hierarchical systems in [17] we will come back to the equal mass non-spinning systems and further displace the initial location of the third hole to coordinates  $(x, y) = (30M, 30M)$  with respect to the center of mass of the inner binary. We have also ensured to have a set of simulations with increasing magnitude of the linear momentum from the quasicircular  $P_{qc}$  at that  $d = 42M$  location by using a factor  $\times(1, 1.5, 2, 3)$  of the original  $P_{qc}(d = 30M)$ , as described in Table V, and labeled them as 3BHscat1-4 respectively. Using as a reference the factor  $1 - f = P_T/P_{qc}$  of the actual tangential linear momentum to the corresponding quasicircular one [35], in the Newtonian approximation  $f < 1 - \sqrt{2}$  would lead to scattering orbits. Thus our first choice would lead to an elliptic orbit and the other three to scattering orbits as we observe in the actual full numerical tracks displayed in Figure 11, where we also observe the triggering of the binary's merger at successive later times. The precise merger times are reported in Table VI and they indicate a correlation between the merger times (corrected by the time of closest approach  $t_{min}$ ) with the closest distance reached by the scattering hole to the binary. The closest the approach, the later the merger (except for the first case  $1P_{qc}$  that leads to a bound elliptic orbit and that at such closest approach prompts an early merger as seen in our former studies [15] of close encounters of three black holes).

This dependence with the closest approach, even for fast moving black holes, somewhat confirm the relevance of the concept of a 'sudden' interaction of third black holes with an inner binary and may be used to develop approximation techniques, for instance of the sort of [36] and references therein.

### B. High mass ratio Three black holes configurations

Interesting astrophysical scenarios involving three black holes involve stellar mass binary interactions in globular clusters [37] with intermediate mass holes at its core [38]. These interactions may lead to eccentricity increase in the binary [39] with implications for the characteristics of the gravitational waves [40]. In order to start exploring these effects during the latest stages of the binary, previous to its merger, we will consider a sequence of increasingly dispair mass ratios of the binary

TABLE V. Initial parameters for equal-mass, non-spinning scattering configurations.

Config	3BHscat1	3BHscat2	3BHscat3	3BHscat4
$x_1/M$	-9.95027835	-9.95027835	-9.95027835	-9.95027835
$y_1/M$	3.96250893	3.96250893	3.96250893	3.96250893
$p_1^x/M$	-0.05705839	-0.05705839	-0.05705839	-0.05705839
$p_1^y/M$	-0.02179566	-0.03250943	-0.04322319	-0.06465073
$m_1^p/M$	0.32406500	0.32392700	0.32352700	0.32272500
$m_1^H/M$	0.33323974	0.33332045	0.33321649	0.33326252
$x_2/M$	-9.95027835	-9.95027835	-9.95027835	-9.95027835
$y_2/M$	-3.96250893	-3.96250893	-3.96250893	-3.96250893
$p_2^x/M$	0.0570813769	0.05708138	0.05708138	0.05708138
$p_2^y/M$	-0.02105940	-0.03177317	-0.04248694	-0.06391447
$m_2^p/M$	0.32406500	0.32392700	0.32352700	0.32272500
$m_2^H/M$	0.33339854	0.33347563	0.33336817	0.33340831
$d/M$	7.92501786	7.92501786	7.92501786	7.92501786
$d_{spd}/M$	10.623675275	10.63025694	10.63841909	10.66317740
$x_3/M$	19.7641253	19.7641253	19.7641253	19.7641253
$y_3/M$	-30.0000000	-30.0000000	-30.0000000	-30.0000000
$p_3^x/M$	-0.00002299	-0.00002299	-0.00002299	-0.00002299
$p_3^y/M$	0.04285506	0.06428260	0.08571013	0.12856519
$m_3^p/M$	0.33008000	0.32925000	0.32815000	0.32506000
$m_3^H/M$	0.33331900	0.33330898	0.33333513	0.33332132

TABLE VI. Merger time, time and distance of closest approach of the inner binary for different values of the initial linear momentum of the third black hole.

Configuration	$t_{merger}/M$	$t_{min}/M$	$D_{min}/M$
$1P_{qc}$	686.94	240.19	15.60
$1.5P_{qc}$	1222.81	164.31	23.82
$2P_{qc}$	1150.69	116.00	26.41
$3P_{qc}$	1072.50	77.90	27.93

(which itself is chosen formed by equal mass nonspinning holes) to a much more massive third hole, modeling an intermediate mass black hole at the core of a globular cluster. We thus start comparing mass ratios a factor eight to each the binary's individual mass black holes 8:1:1 and then raise it to an eighteen mass ratio 18:1:1 as displayed in Table VII. We considered coplanar orbits prograde and retrograde with respect to the larger hole labeled as 3BH1q and 3BH2q respectively. Figure 12 displays the orbital motion of the three holes as seen in the center of mass frame for the 3BH2q8 configuration. The binary merges at about completing an orbit around the larger hole. The bottom plot tracks the center of mass of the binary, with an expected follow up slow decay around the larger hole (and eccentricity), product of the gravitational radiation mostly at low frequencies, while the merging of the binary itself contributing mostly at higher gravitational waves frequencies (although, of course, the three body system radiates as a whole).

The sequence of increasing mass ratios can be followed, but we found the trends of binary's merger times to be already clear. In fact, Figure 13 displays a pattern of increased merger time with the increase of the mass ratio, as expected due to the lower efficiency of gravita-

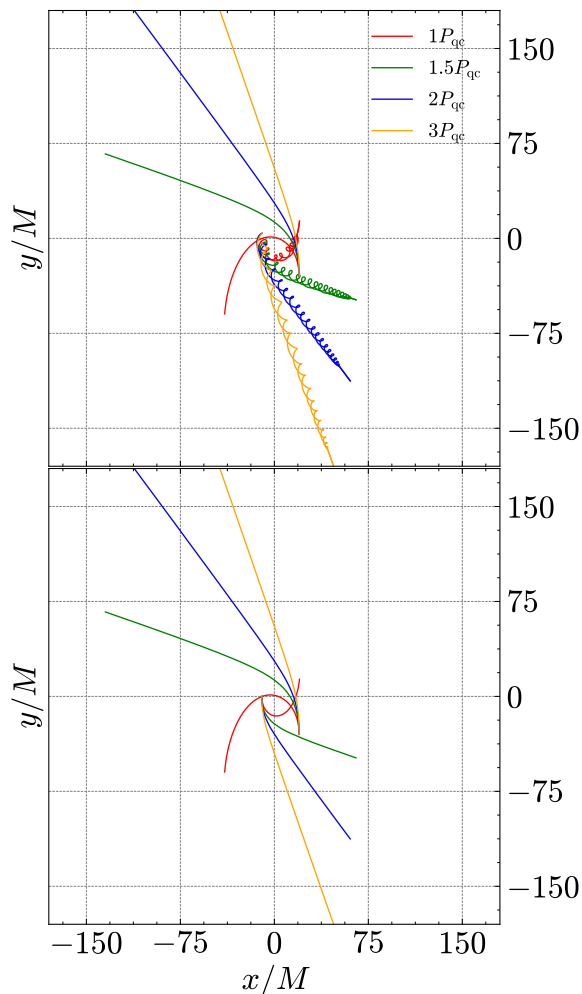


FIG. 11. Trajectories of the binary until merger with the third black hole starting at the same distance  $D = 42M$  but with increasing linear momentum used for the quasicircular previous cases by factors  $\times 1, 1.5, 2, 3$ . Below the trajectory of the binary's center of mass and the third black hole.

tional radiation relative to the total mass of the system with respect to the equal mass cases 3BH1q1 and 3BH2q1 (that we also include in the study to serve as a reference). We also note the relative delay for each of the mass ratios between their corresponding prograde and retrograde configurations. Notably the retrograde cases delay their merger with respect to the prograde possibly due to its shortest duration close approach interactions with the larger third black hole. An effect further supporting the notion of the 'sudden' interaction predominance in three black hole configurations. Precise times and number of orbits to merger are compiled in Table VIII. We also note here that this reverses the sense of the hangup effect [41, 42] observed in binary systems with spins, where spins aligned with the orbital angular momentum lead to a merger delay and antialigned spins to a prompt merger.

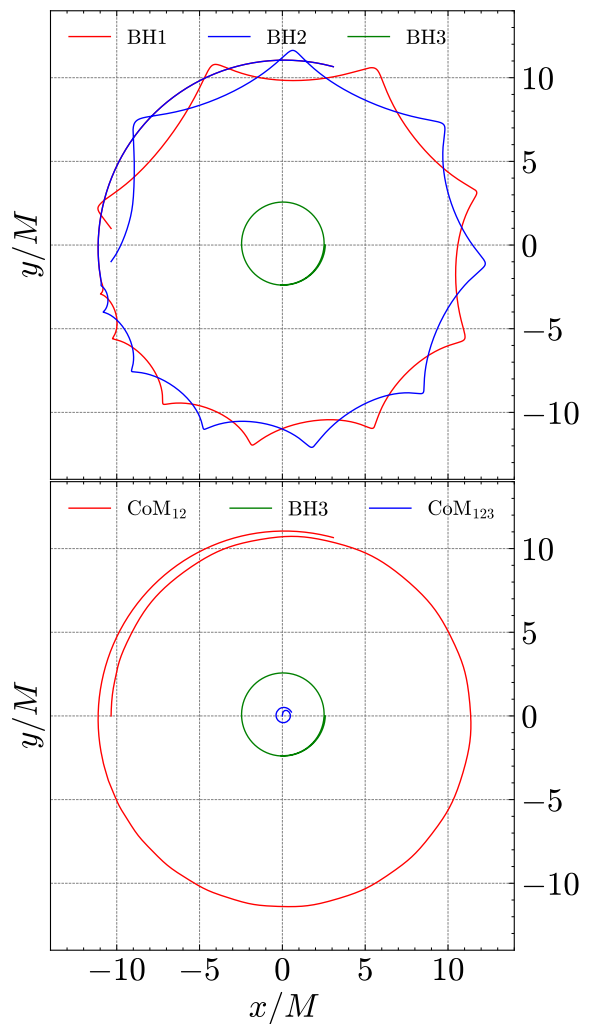


FIG. 12. The hierarchical orbits of the three black holes in the center of mass frame (see also lower panel) for the 8:1:1 unequal mass 3BH2q8 configuration. The binary center of mass is moving clockwise in the figure while the binary itself the opposite.

## VI. CONCLUSIONS AND DISCUSSION

Our full analytic approach to solve perturbatively (Bowen-York) initial data for three black holes is naturally limited by the smallness of the expansion parameters, namely spins and linear momenta of the holes, as well as the inverse of its initial separation. While the last two parameters are often times small, the extension to highly spinning black holes shows inaccuracies. To cure those we have implemented a hybrid approach solving the inner binary with high spins fully numerically, in the usual way with the TwoPunctures solver of the Hamiltonian constraint, and then add up the analytic expansion of the third hole contribution. We validated this hybrid procedure in the small spin regime and the whole procedure proved accurate enough for our current exploratory

TABLE VII. Initial parameters for non-spinning coplanar setups with mass ratios  $m_3^H : m_2^H : m_1^H$  of 1:1:1, 8:1:1 and 18:1:1.

Config	3BH1q1	3BH2q1	3BH1q8	3BH2q8	3BH1q18	3BH2q18
$x_1/M$	-9.95121484	-9.98358508	-10.3327592	-10.341799	-10.758263	-10.760757
$y_1/M$	3.29853493	3.29853493	0.98956048	0.98956048	0.49478024	0.49478024
$p_1^x/M$	-0.06462839	-0.06462736	-0.01930654	-0.01930063	-0.00965915	-0.00965788
$p_1^y/M$	-0.02218703	0.02128140	-0.02595764	0.02601309	-0.01544532	0.01538831
$m_1^p/M$	0.32205500	0.32205500	0.09380000	0.09380000	0.04650000	0.04650000
$m_1^H/M$	0.33335970	0.33335041	0.09997350	0.09998022	0.04997869	0.04997759
$x_2/M$	-9.95121484	-9.98358508	-10.3327592	-10.341799	-10.758263	-10.760757
$y_2/M$	3.29853493	3.29853493	-0.98956048	0.98956048	-0.49478024	0.49478024
$p_2^x/M$	0.06465142	0.06465244	0.01947740	0.01948331	0.00973282	0.00973409
$p_2^y/M$	-0.02082070	0.02264774	-0.02554774	0.02642299	-0.01524037	0.01559326
$m_2^p/M$	0.32205500	0.32205500	0.09380000	0.09380000	0.04650000	0.04650000
$m_2^H/M$	0.33334372	0.33336827	0.09996202	0.10000287	0.04997149	0.04998916
$d/M$	6.59706986	6.59706986	1.97912096	1.97912096	0.98956048	0.98956048
$d_{spd}/M$	9.19569237	9.19583305	2.88313183	2.88384645	1.45922435	1.45947139
$x_3/M$	19.9428396	19.9121871	2.59715370	2.58932285	1.20318845	1.20106818
$y_3/M$	0.00000000	0.00000000	0.00000000	0.00000000	0.00000000	0.00000000
$p_3^x/M$	-0.00002303	-0.00002508	-0.00017086	-0.00018268	-0.00007367	-0.00007621
$p_3^y/M$	0.04300773	-0.04392914	0.05150537	-0.05243609	0.03068568	-0.03098158
$m_3^p/M$	0.32911500	0.32906500	0.79320000	0.79320000	0.89620000	0.89620000
$m_3^H/M$	0.33336348	0.33334239	0.79961960	0.79964496	0.90002248	0.90002969
$M\Omega$	0.00582575	0.00586644	0.01925963	0.01938382	0.02139540	0.02147362
$D/M$	29.8940544	29.89577218	12.9299129	12.9311219	11.9614515	11.9618252

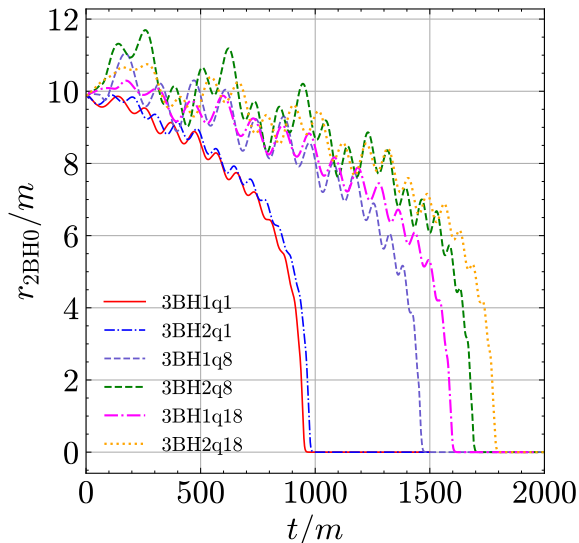


FIG. 13. The time evolution of the binary’s separation  $d = r_{2BH0}/m$  displays the eccentricity effects triggered by the third (more massive) black hole and the merger delay due to the smaller mass ratio and the orientation of the orbit.

studies. We also refer to the convergence studies and more details of the analytic and numerical techniques to the previous paper [17] in this series.

We then revisited the triple black hole scenario to study their merging times and eccentricity evolution in the presence of spins. We found that the third black hole delays the merger of the spinning binary by an inverse a power of the distance,  $\sim 1/D^{1.6}$ . This behavior is clearly

TABLE VIII. Number of orbits to merger and merger time of the inner binary for different mass ratios with the third black hole. Merger time is normalised by the total mass of each inner binary  $m$ . Cases 3BH1-2q1-8-18

Configuration	#orbits	$t_{\text{merger}}/m$
3BH1q1	6.51	945.66
3BH2q1	6.62	972.28
3BH1q8	7.58	1461.25
3BH2q8	8.02	1688.75
3BH1q18	5.75	1595.00
3BH2q18	6.35	1785.00

different to those of the nonspinning configurations studied in our previous work [17], that was  $\sim 1/D^{2.5}$ . While we interpreted the nonspinning three black hole interactions dominated by tidal effects, now in the spinning case we interpret this leading interaction as being dominated by a sort of spin-orbit effect (scaling like  $\sim 1/D^{1.5}$ ), taking place during the closest approach and for a short term, namely a “sudden” interaction of the third hole with the closest hole of the binary at that moment. We also observe here that if we start the third black hole closer to  $\approx 30M$  this leads to a prompt disruption and a binary or merger as observed in previous work [15, 17].

This interesting new dependence of the merger time with the distance of the third hole to the binary in the presence of the spin interactions prompted the study of scattering configurations of the third hole to study its effects on triggering merger and eccentricity on inner binaries to check the idea of the “sudden” interaction as the leading effect. In fact, we verified a dependence of

the merger times with the scattering closest approach distance to the binary as described in Sec. V A, even for nonspinning holes. These effects have the potential to display distinctive features, for instance, gravitational waves from the scattering of two black holes have been studied in [43] and its detectability in [44].

Finally, we have also studied the mass ratio dependence on the inner binary orbiting a much larger third black hole. This could be a prototypical study for a stellar masses black hole binary near a central intermediate mass hole in a globular cluster. Our explicit studies are for mass ratios 8:1:1 and 18:1:1, but the sequence could be continued for at least until 128:1:1 systems, since we have proven our full numerical evolution techniques work very well [24] applied to binary black holes holding such small mass ratios.

## ACKNOWLEDGMENTS

The authors thank Alessandro Ciarfella, James Healy, Hiroyuki Nakano, and Yosef Zlochower for useful dis-

cussions. The authors also gratefully acknowledge the National Science Foundation (NSF) for financial support from Grant PHY-2207920. Computational resources were also provided by the Blue Sky, Green Prairies, and White Lagoon clusters at the CCRG-Rochester Institute of Technology, which were supported by NSF grants No. AST-1028087, No. PHY-1229173, No. PHY-1726215, and No. PHY-2018420. This work used the ACCESS allocation TG-PHY060027N, founded by NSF, and project PHY20007 Frontera, an NSF-funded Petascale computing system at the Texas Advanced Computing Center (TACC).

- 
- [1] J. D. Schnittman and J. H. Krolik, *Astrophys. J.* **806**, 88 (2015), arXiv:1504.00311 [astro-ph.HE].
- [2] C. Nixon, *Mon. Not. Roy. Astron. Soc.* **423**, 2597 (2012), arXiv:1204.4185 [astro-ph.HE].
- [3] F. Antonini and H. B. Perets, *Astrophys. J.* **757**, 27 (2012), arXiv:1203.2938 [astro-ph.GA].
- [4] J. Samsing, M. MacLeod, and E. Ramirez-Ruiz, *Astrophys. J.* **784**, 71 (2014), arXiv:1308.2964 [astro-ph.HE].
- [5] M. Bonetti, F. Haardt, A. Sesana, and E. Barausse, *Mon. Not. Roy. Astron. Soc.* **477**, 3910 (2018), arXiv:1709.06088 [astro-ph.GA].
- [6] V. Gayathri, J. Healy, J. Lange, B. O'Brien, M. Szczepanczyk, I. Bartos, M. Campanelli, S. Klimentko, C. O. Lousto, and R. O'Shaughnessy, *Nature Astron.* **6**, 344 (2022), arXiv:2009.05461 [astro-ph.HE].
- [7] J. Shapiro Key and N. J. Cornish, *Phys. Rev. D* **83**, 083001 (2011), arXiv:1006.3759 [gr-qc].
- [8] D. J. D'Orazio and J. Samsing, *Mon. Not. Roy. Astron. Soc.* **481**, 4775 (2018), arXiv:1805.06194 [astro-ph.HE].
- [9] B.-M. Hoang, S. Naoz, B. Kocsis, W. Farr, and J. McIver, *Astrophys. J.* **875**, L31 (2019), arXiv:1903.00134 [astro-ph.HE].
- [10] A. Sesana, *Phys. Rev. Lett.* **116**, 231102 (2016), arXiv:1602.06951 [gr-qc].
- [11] S. Vitale, *Phys. Rev. Lett.* **117**, 051102 (2016), arXiv:1605.01037 [gr-qc].
- [12] E. Barausse, N. Yunes, and K. Chamberlain, *Phys. Rev. Lett.* **116**, 241104 (2016), arXiv:1603.04075 [gr-qc].
- [13] M. Bonetti, A. Sesana, E. Barausse, and F. Haardt, *Mon. Not. Roy. Astron. Soc.* **477**, 2599 (2018), arXiv:1709.06095 [astro-ph.GA].
- [14] M. Bonetti, A. Sesana, F. Haardt, E. Barausse, and M. Colpi, *Mon. Not. Roy. Astron. Soc.* **486**, 4044 (2019), arXiv:1812.01011 [astro-ph.GA].
- [15] C. O. Lousto and Y. Zlochower, *Phys. Rev. D* **77**, 024034 (2008), arXiv:0711.1165 [gr-qc].
- [16] M. Campanelli, C. O. Lousto, P. Marronetti, and Y. Zlochower, *Phys. Rev. Lett.* **96**, 111101 (2006), gr-qc/0511048.
- [17] G. Ficarra, A. Ciarfella, and C. O. Lousto, *Phys. Rev. D* **108**, 064045 (2023), arXiv:2308.07365 [gr-qc].
- [18] Y. Zlochower, J. G. Baker, M. Campanelli, and C. O. Lousto, *Phys. Rev. D* **72**, 024021 (2005), arXiv:gr-qc/0505055.
- [19] S. Brandt and B. Brügmann, *Phys. Rev. Lett.* **78**, 3606 (1997), gr-qc/9703066.
- [20] M. Ansorg, B. Brügmann, and W. Tichy, *Phys. Rev. D* **70**, 064011 (2004), gr-qc/0404056.
- [21] J. Thornburg, *Class. Quant. Grav.* **21**, 743 (2004), gr-qc/0306056.
- [22] M. Campanelli, C. O. Lousto, Y. Zlochower, B. Krishnan, and D. Merritt, *Phys. Rev. D* **75**, 064030 (2007), gr-qc/0612076.
- [23] E. Schnetter, S. H. Hawley, and I. Hawke, *Class. Quant. Grav.* **21**, 1465 (2004), gr-qc/0310042.
- [24] C. O. Lousto and J. Healy, *Phys. Rev. Lett.* **125**, 191102 (2020), arXiv:2006.04818 [gr-qc].
- [25] M. Campanelli and C. O. Lousto, *Phys. Rev. D* **59**, 124022 (1999), arXiv:gr-qc/9811019 [gr-qc].
- [26] C. O. Lousto and Y. Zlochower, *Phys. Rev. D* **76**, 041502(R) (2007), gr-qc/0703061.
- [27] J. M. Bowen and J. W. York, Jr., *Phys. Rev. D* **21**, 2047 (1980).
- [28] P. Galaviz, B. Bruegmann, and Z. Cao, *Phys. Rev. D* **82**, 024005 (2010), arXiv:1004.1353 [gr-qc].
- [29] S. Bai, Z.-J. Cao, W.-B. Han, C.-Y. Lin, H.-J. Yo, and J.-P. Yu, *J. Phys. Conf. Ser.* **330**, 012016 (2011), arXiv:1203.6185 [gr-qc].
- [30] M. Imbrogno, C. Meringolo, and S. Servidio, *Class. Quant. Grav.* **40**, 075008 (2023), arXiv:2108.01392 [gr-

- qc].
- [31] J. Healy, C. O. Lousto, H. Nakano, and Y. Zlochower, *Class. Quant. Grav.* **34**, 145011 (2017), arXiv:1702.00872 [gr-qc].
  - [32] C. J. Woodford, M. Boyle, and H. P. Pfeiffer, *Phys. Rev. D* **100**, 124010 (2019), arXiv:1904.04842 [gr-qc].
  - [33] J. Healy and C. O. Lousto, *Phys. Rev. D* **102**, 104018 (2020), arXiv:2007.07910 [gr-qc].
  - [34] M. Campanelli, C. O. Lousto, H. Nakano, and Y. Zlochower, *Phys. Rev. D* **79**, 084010 (2009), arXiv:0808.0713 [gr-qc].
  - [35] A. Ciarfella, J. Healy, C. O. Lousto, and H. Nakano, *Phys. Rev. D* **106**, 104035 (2022), arXiv:2206.13532 [gr-qc].
  - [36] P. Rettengo, G. Pratten, L. M. Thomas, P. Schmidt, and T. Damour, *Phys. Rev. D* **108**, 124016 (2023), arXiv:2307.06999 [gr-qc].
  - [37] K. Gultekin, M. C. Miller, and D. P. Hamilton, *AIP Conf. Proc.* **686**, 135 (2003), astro-ph/0306204.
  - [38] M. C. Miller and E. Colbert, *Int.J.Mod.Phys. D* **13**, 1 (2004), arXiv:astro-ph/0308402 [astro-ph].
  - [39] M. Dall’Amico, M. Mapelli, S. Torniamenti, and M. A. Sedda, *Astron. Astrophys.* **683**, A186 (2024), arXiv:2303.07421 [astro-ph.HE].
  - [40] D. M. Pina and M. Gieles, (2023), arXiv:2308.10318 [astro-ph.GA].
  - [41] M. Campanelli, C. O. Lousto, and Y. Zlochower, *Phys. Rev. D* **74**, 041501(R) (2006), gr-qc/0604012.
  - [42] J. Healy and C. O. Lousto, *Phys. Rev. D* **97**, 084002 (2018), arXiv:1801.08162 [gr-qc].
  - [43] R. M. O’Leary, B. Kocsis, and A. Loeb, *Mon. Not. Roy. Astron. Soc.* **395**, 2127 (2009), arXiv:0807.2638 [astro-ph].
  - [44] S. Mukherjee, S. Mitra, and S. Chatterjee, *Mon. Not. Roy. Astron. Soc.* **508**, 5064 (2021), arXiv:2010.00916 [gr-qc].